Shahrood University of Technology
Iranian Society of Mining Engineering (IRSME)
Journal of Mining and Environment (JME)
journal homepage: www.jme.shahroodut.ac.ir
THOMSON REUTERS
Vol. 10, No. 2, 2019, 529-541.
DOI: 10.22044/jme.2019.7978.1673

Efficiency of seismic wave velocity and electrical resistivity in estimation of limestone rock mass quality indices (Q , Q_{srm}) (Case study: Asmari formation, SW Iran)

S.M. Fatemi Aghda*, M. Kianpour and M. Talkhablou

Department of Geology, Kharazmi University, Tehran, Iran

Received 4 February 2019; received in revised form 23 February 2019; accepted 9 March 2019

Keywords

Sedimentary Rock Mass Quality Index

Asmari Limestone

Geophysical Method

Karstification

Empirical Equations

Fuzzy Inference System

Abstract

In this work, the relationship between the P-wave velocity (V_p) and the Electrical Resistivity (ER) parameters with rock mass quality indices is investigated; parameters such as rock mass quality classification (Q) and modified system for sedimentary rocks (Q_{srm}). For making predictive models, about 1200 data-sets were extracted from sections drilled in Seymareh and Karun 2 Dam Sites (SDS and KDS) in Asmari Formation, SW Iran. The statistical and fuzzy methods were used to study the relationships between the geophysical parameters and the rock mass quality. Since in the Q_{srm} classification, the existence of cavities; and layering and rock texture are considered in addition to the parameters considered in the Q classification; it provides a better description of rock mass and is closely related to parameters V_p and ER. The equations obtained for predicting Q and Q_{srm} showed the determination coefficients (R^2) to be 0.48 and 0.67, respectively, and the coefficient of determination 0.86 for Q_{srm} was calculated by the fuzzy model. Finally, Mean Absolute Deviation (MAD), Variance Accounted For (VAF), and Root Mean Square Error (RMSE) were used to check the prediction performance of the statistical and fuzzy methods. The results of the calculated errors also showed that the fuzzy models were interesting because they had a good accuracy for predicting Q_{srm}. In addition, by increasing the degree of karstifiction, the efficiency of the geophysical method for estimation of Q decreased rapidly, which was due to ignoring the cavities in this category.

1. Introduction

A knowledge of rock mass quality indices; in different aspects; is an important prerequisite in designing the civil engineering and mining activities. Numerous researchers have developed rock mass classification systems. One of the first systems to be developed is the Rock Quality Designation (RQD) system [1]. This system only accounts for the frequency of jointing within a rock mass. Later systems; such as the Rock Mass Rating (RMR) [2] and Q systems [3]; not only use RQD as one of their measurable parameters; but also include factors such as the intact rock strength, joint spacing, joint condition, field stress, number of joint sets, and effects of groundwater. In addition to the traditional Q system, this research work refers to Q_{srm}. Compared with Q, Q_{srm} has four other factors (Equation 1 [4]).

$$Q_{srm} = \frac{RQD}{J_n} \times \frac{J_r}{J_a} \times \frac{J_w}{SRF} \times \frac{R_s}{S} \times \frac{T}{V} \quad (1)$$

Corresponding author: fatemi@khu.ac.ir (S.M. Fatemi Aghda).

where, R_s is the rating for the bedding, S is the rating for dipping of the layers, T is the rating for the texture of the rock mass, and V is the rating for the presence of cavities.

Today, in the engineering projects such as mining projects, engineering geology, and civil engineering, seismic P-wave velocity (V_p) and Electrical Resistivity (ER) are widely used for rock mechanic applications [4-7]. V_p and ER are both functions of rock mass properties [8]. In particular, V_p and ER are now the standard parameters that can give useful information [6-9]. The correlation between V_p and ER with the characteristics of rocks is well known and has been described in a number of textbooks and studies. Sojren et al. [9] correlated P-wave velocity with mechanical rock parameters such as fracture frequencies and RQD. Boadu and Long [10] proposed a fracture model called "Modified Displacement Discontinuity" (MDD) for seismic wave propagation in fractured media. The model takes into account the fracture size, fraction of surface areas in contact, viscosity of infill material, and fracture aperture. Boadu [11] studied empirical least squares regression relationships between the seismic wave velocity and the permeability and rock mass properties. Barton [12] proposed an empirical correlation between the Q factor and P-wave velocity based on the data from hard rock tunneling projects in several countries. In addition, others [13-17] conducted many other studies for correlation between the rock mass quality and geophysical parameters. These studies also highlighted some of the factors that may affect the relationships such as rock type, mineral content, grain size, cavities, and factors associated with increasing depth. However, research to assess the rock mass quality is still one of the hardest tasks of the researchers, and the empirical models used to predict rock mass quality are often mathematical and cannot be generalized to all areas. This makes choosing the equations difficult. In addition, Q_{srm} has rarely been calculated and investigated in Iran's geological zones like other regions. The purpose of this work was to check the geophysical experiments and degree of karstification to predict the Asmari limestone quality indices such as rock mass quality (Q) [3] and modified sedimentary rock mass quality (Q_{srm}) [4]; in SW Iran.

In this work, to obtain the geophysical and geotechnical data, the 3D GIS information layers from V_p, ER, Q and Q_{srm} were created by interpolation between the data extracted from the location of galleries and drilling boreholes. All data-point sets were obtained from galleries and drilled boreholes at Karun 2 and Seymareh Dam Sites (KDS and SDS) in SW Iran. Finally, using the multivariate regression method and fuzzy method (FIS), models for predicting Q and Q_{srm} in Asmari limestone were presented. In total, about 1200 data-point sets were used for modeling, and V_p and ER were considered as the independent parameters. Figure 1 shows the general principles of this research work. The results of FIS and multivariate regression show that combinations of ER and V_p; in cases where geotechnical studies are not possible, can give a good estimation of the Asmari limestone stability parameters that have a great effect on the Q_{srm} index. In addition, due to consideration of the cavities in the Q_{srm} index, with an increase in the karstification degree, the efficiency of the geophysical methods for prediction of Q_{srm} increases, as compared to Q.

The results obtained can be used for the same geological formation for each region, but similar patterns can be obtained for other areas as well.

2. Geological background of studied areas

The main studied areas are KDS and SDS. KDS is on the Karun River, which is originated from the Zard-Kuh Mountains in the Zagros area, Iran. SDS is on the Seymareh River and its site belongs to the Zagros Mountains in the SW Iran (Figure 2). Geologically, the Sequence stratigraphic rocks of the studied areas; include limestone and marl-limestone; belonging to the Asmari formation (Oligocene-Miocene), Gypsume belongings to the Gachsaran formation (Mio-plocene), and Conglomerate belonging to Bakhtiari formation (Pleo-pleistocene, conglomerate) [18, 19].

Among the different formations in the Zagros region, the Asmari limestone with unique characteristics such as hardness and morphology is suitable for the dam projects in the Zagros area. However, this formation also has some degrees of expansion of karstic cavities that are very effective on the rock mass quality. The formation in its parts includes lime, dolomite-

limestone, and limestone. It deposited during the late Oligocene -early Miocene [20].

The Asmari formation can be divided into three different units based on the formation conditions and the forming rocks as follow:

Upper Asmari (A.3) as 150 m in thickness, moderate to thin bedding, crystal, biologic, and marl limestone; Middle Asmari (As.2) as 150 m in thickness, thick bedding and karstified rocks, massive and dolomitic and marl-limestone; and finally, lower Asmari (As.1) as 188 m in thickness, medium and thick bedding, marl and microcrystalline limestone [21-23]. The limestone rocks studied in this work cover almost all units of the Asmari formation, and consist of high-quality limestone to low calcareous rocks with karstic cavities.

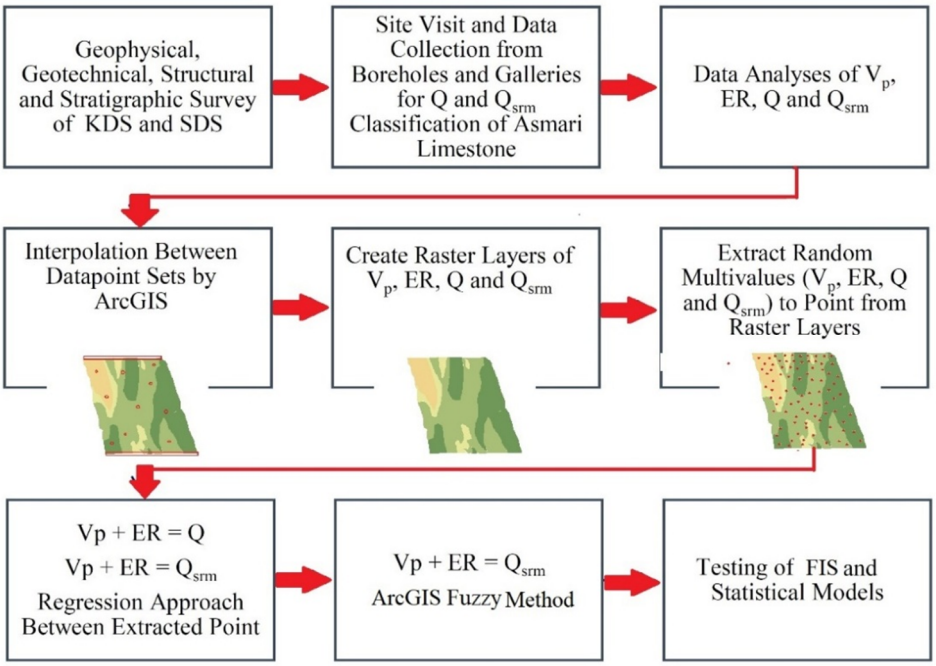

Figure 1. Flowchart of the methods, used in this research; work to evaluate the rock mass quality.

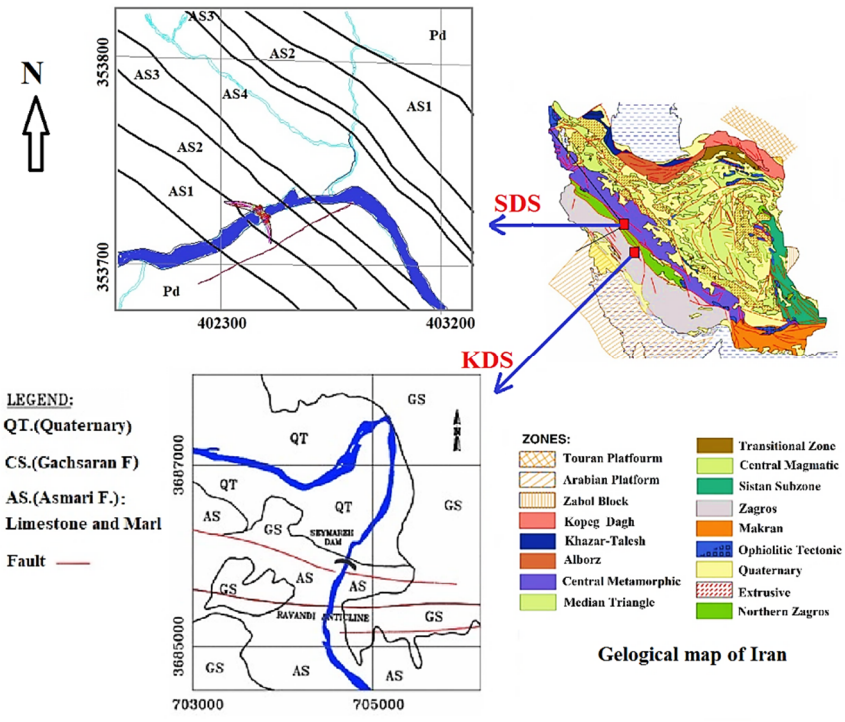

Figure 2. Geological map of SDS and KDS [16, 17].

3. Materials and methods

Recent geophysical works in civil engineering have mostly focused on the parameters V_p and ER [8]. In SDS and KDS, geophysical investigations have been carried out by performing the tomography method of V_p and ER. The main purpose of the geophysical investigations was to assess the quality of rock mass at the valley of dam sites and to investigate the presence of the probable weak zones, identifying anomalies such as crushed zone and cavity. Tomography was performed by cross-gallery (or boreholes) arrangement in sites with a source/receiver spacing of 2 m [18, 19]. Figure 3 shows the location of the ER profiles, galleries, and the studied boreholes between them in SDS and KDS, 3D geometry of seismic geophysical data acquisition in galleries, and boreholes and location of source and receivers in gallery boreholes (E).

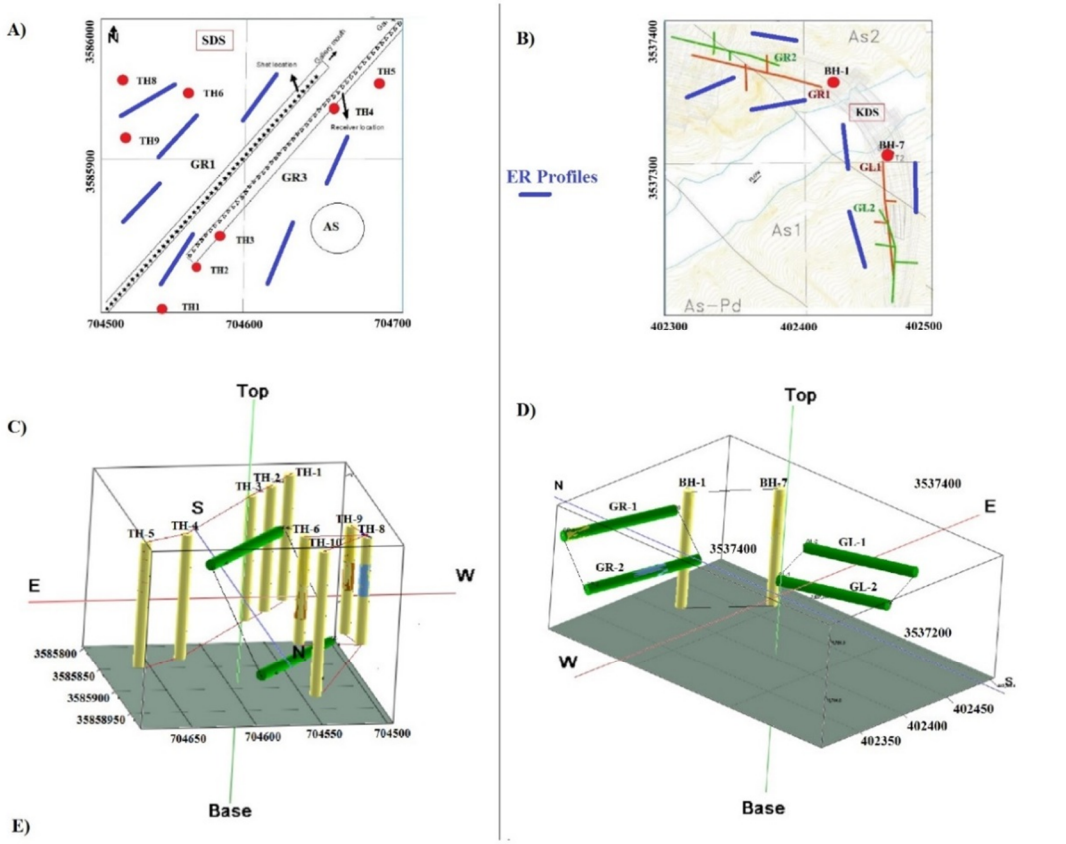

Site Area	Location of receiver Min & max depth, m	Location of source Min & max depth, m	No of file	No of seismograph	Type of source
SDS	TTH2 ‹152-44	TTH1 ‹172-40	71	852	sparker
	TTH3 ‹160-44	TTH2 ‹172-40	46	768	Sparker
	TTH3 ‹142-44	TTH4 ‹142-40	50	600	Sparker
	TTH5 ‹148-44	TTH4 ‹152-40	56	672	Sparker
	TTH6 ‹459-46	TTH10 ‹162-40	67	804	Sparker
	TTH6 ‹160-46	TTH8 ‹162-40	68	816	Sparker
	TTH10 ‹172-46	TTH8 ‹172-40	68	816	Sparker
	TTH9 ‹162-46	TTH8 ‹162-40	67	804	Sparker
	GR1	GR3	80	1600	Explosion
KDS	BH1	BH7	85	1800	Explosion
	GL1	GL2	90	2010	Explosion
	GR1	GR2	80	1600	Explosion

Figure 3. Location of ER profiles, galleries, and studied boreholes between them in SDS (a) and KDS (b), 3D geometry of seismic geophysical data acquisition in galleries and boreholes (C and D), and location of source and receivers in gallery boreholes (E).

For applying the Q and Q_{srm} classification systems on the rock mass classes in SDS and KDS, a site visit was arranged, and the Q and Q_{srm} classification systems were calculated for classifying the drill-cores and rock sections of the selected boreholes and galleries, drilled in different rock units from AS-1 (oldest) to AS-3 (youngest). The Q and Q_{srm} indices were calculated in the TH1 to TH9 boreholes, GR1 and GR3 galleries in SDS and in BH1, BH7 boreholes and GR1, GR2, GL1, and GL2 galleries in KDS, and in boreholes drilled between them. The results of the preliminary Q and Q_{srm} classifications are presented in Figure 4. Looking at this figure, the Q values confirm the very poor to good quality, and the Q_{srm} values confirm the very poor to fair quality of the studied rock masses.

In addition, using the GIS method, for acquiring the geophysical and geotechnical data, we made it possible to carry out 3D raster layers of the V_p, ER, Q, and Q_{srm} sections by the interpolation methods. All the created GIS raster layers of rock mass quality and geophysical parameters are shown in Figures 5 and 6. In Figure 5, four sections of the information layers obtained in SDS are shown. At the GR1-GR3 section, the information layers are derived from the interpolation of data taken in galleries and several boreholes drilled between them. In this section, the map of a small anomaly has an 80-degree slope and is related to a faulted zone. Furthermore, at the TH1-TH2 section, some anomalies were observed, beginning with a depth of 100 m up to the depths and levels of 543, 518, and 590 m in the TH3-TH4 section. The anomaly observed in the level of 590 m in the TH4 boreholes were located near the water level and extended to the TH3 borehole. The small anomalies in TH4 and TH5 at levels of 589, 526, and 510 m are related to small set joints. A big anomaly was clearly seen at levels of 570 to 597 m of the TH8-TH9 section. In the TH6-TH10 and TH6-TH8 sections, the quality of rock was good and proved that with increasing depth, velocity decreased. The information layers of Figure 6 are also derived from the data interpolation between the GR1-GR2 and GL1-GL2 galleries and BH1-BH7 boreholes in KDS. Anomalies in the GR1-GR2 galleries were related to set joints, and in GL1-GL2, the galleries were related to faults and joints. In addition, in the BH1-BH7 section, anomaly was clearly seen at levels of 560 to 575 m.

3.1. Correlation between Q, Q_{srm} with ER and V_p

A detailed comparison of the V_p and ER sections with the corresponding rock mass quality maps (at the same scale) was performed. By extracting about 1200 sets of data from raster layers using multi-values of point technique in ArcGIS, the samples and multivariate regression analyses were developed for the Q and Q_{srm} recorded values (dependent variables) with V_p and ER (independent variables). Figure 7 shows a matrix plot of the sample regression analyses and the important relationships V_p *vs.* Q_{srm} ($R^2 = 0.52$), V_p *vs.* Q ($R^2 = 0.42$), ER *vs.* Q_{srm} ($R^2 = 0.34$), and ER *vs.* Q ($R^2 = 0.29$) are presented. It is clear that the geophysical parameters show the best relationships with the Q_{srm} index.

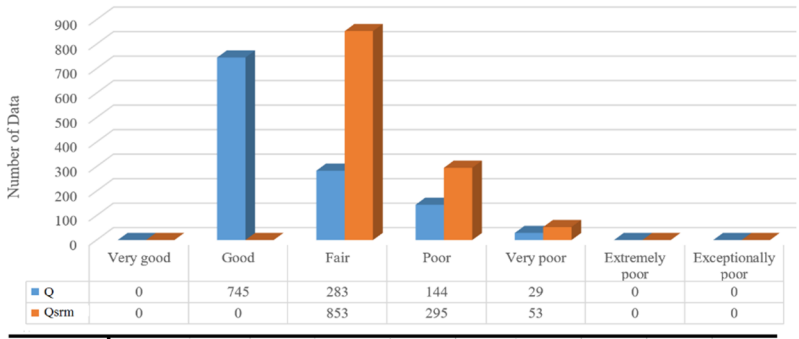

Parameter	RQD%	J_n	J_r	J_a	J_w	SRF	R_s	S	T	V
Range	15-90	9-15	0.5-2	0.75-8	0.2-1	1-10	0.5-1	0.5-5	0.5-2	0.5-5

Figure 4. The range of Q and Q_{srm} quantities of the studied calcareous rock masses and relative parameters.

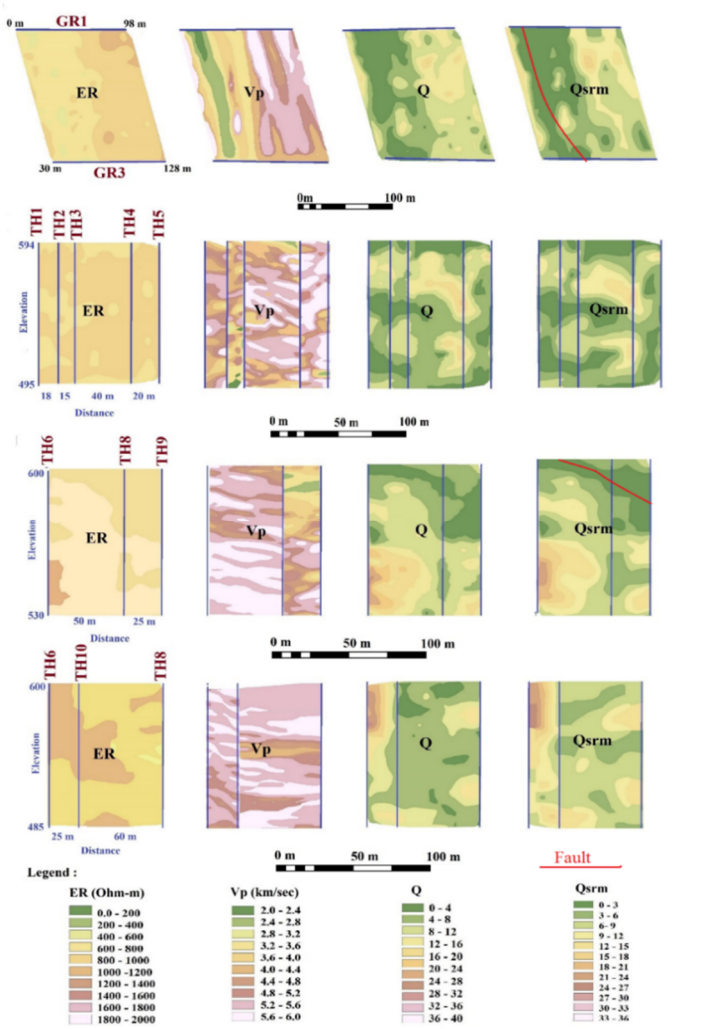

Figure 5. Geophysical, Q and Q_{srm} raster layers in SDS.

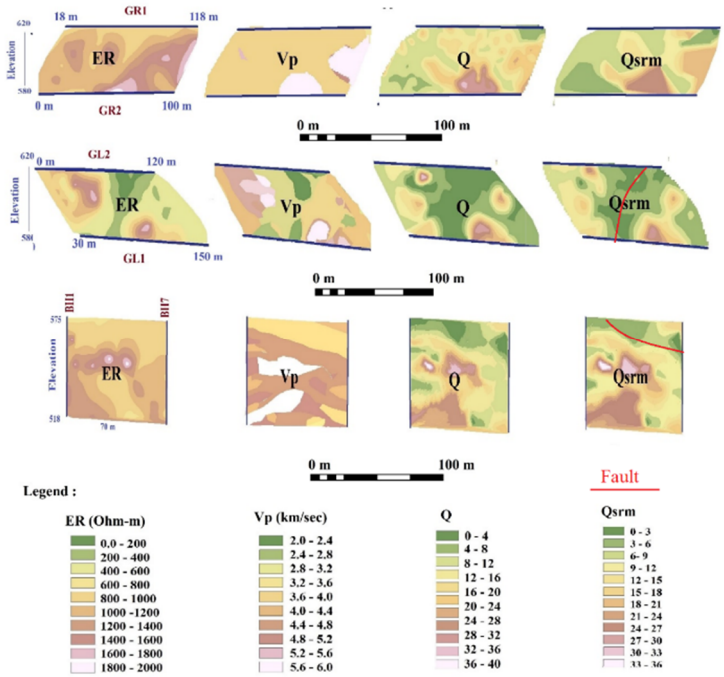

Figure 6. Geophysical, Q and Q_{srm} raster layers in KDS.

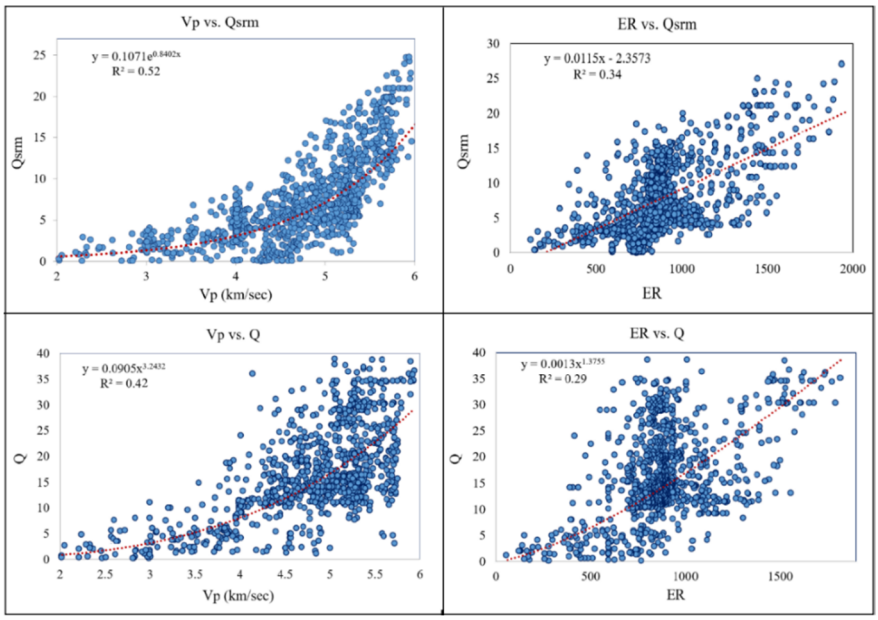

Figure 7. Regression analyses of relation between V_p, ER, Q and Q_{srm}.

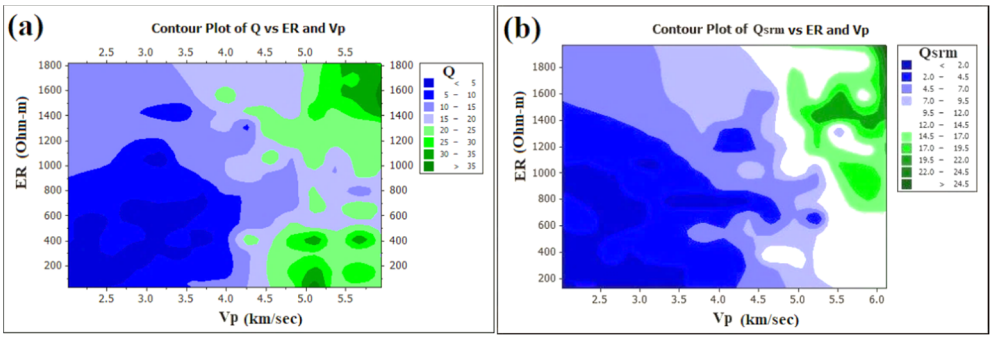

Figure 8. Contour plots of relation between V_p and ER with Q (a) and Q_{srm} (b).

Figure 8 shows a schematic image of the contour plot of relation between V_p and ER with Q and Q_{srm}. As shown in Figures 8(a) and 8(b), the one obtained based on Q_{srm} has the highest determination. In fact, increasing the V_p and ER parameters simultaneously, the Q_{srm} index with a regular trend increases but the trend of change in the Q index is accompanied by some anomaly.

The best fit obtained multivariate equations to estimate Q and Q_{srm} are written as Equations 2 and 3, respectively (Figure 9). The results obtained show that the best equation between V_p and ER with Q_{srm} (R^2 = 0.67) is more reliable than the best between V_p and Q (R^2 = 0.48).

$$Q_{srm} = 26.6545 - 16.1988 \times V_p + 2.31 \times {V_p}^2 + 0.005289 \times ER \qquad R^2 = 0.67 \quad (2)$$

$$Q = -19.957 - 0.01985 \times ER + 0.0000105 \times ER^2 + 10.112 \times V_p - 0.288 \times {V_p}^2 \qquad R^2 = 0.48 \quad (3)$$

Figure 10 shows comparison between the measured and predicted Q and Q_{srm} upon the base of Equations 2 and 3. In the karstic samples, the difference in error and the predicted values by equations 2 and 3 showed more differences with each other. Figure 11 shows the contour map of the values of Q_{srm}, difference of error percentage, and degree of karstification. As shown in this figure, an increase in the difference between the values predicted by Equations 2 and 3 and the drop in the Q_{srm}, indicates the degree of karstification of the rock. The geological reason for this is to consider cavities as parameter V in the Q_{srm} classification. V indicates the presence of cavities in the rock mass, their density, and the filling of the cavities with clay or other materials.

Certainly, the presence of cavities and their properties have a great influence on the geophysical parameters but it not considered in the Q classification. Therefore, the efficiency of the Q_{srm} index increases significantly compared to Q by increasing the degree of karstification.

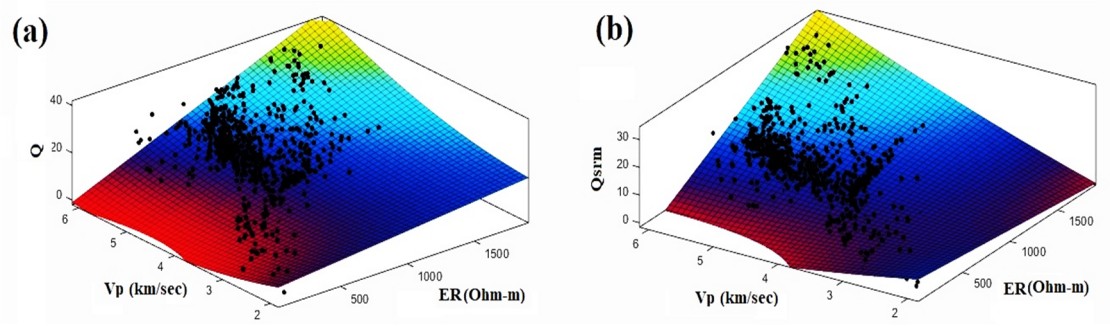

Figure 9. Multivariate relation between V_p and ER with Q (a) and Q_{srm} (b).

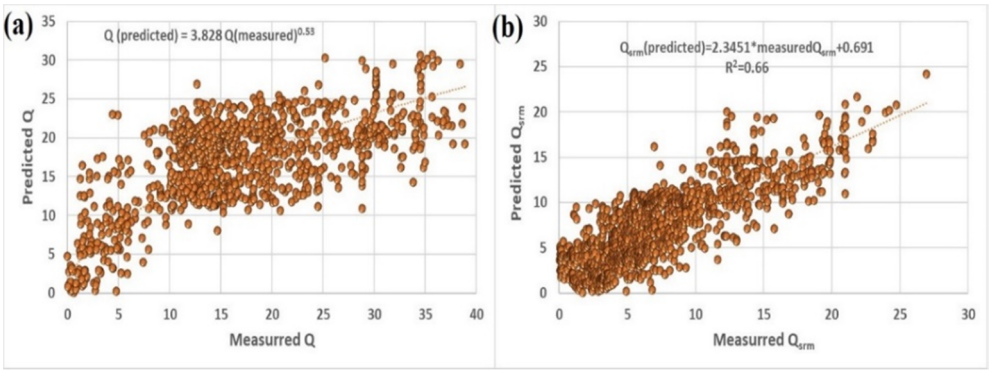

Figure 10. The best-fit line determined between predicted Q (a) and Q_{srm} (b) from multivariate regression analyses and measured values.

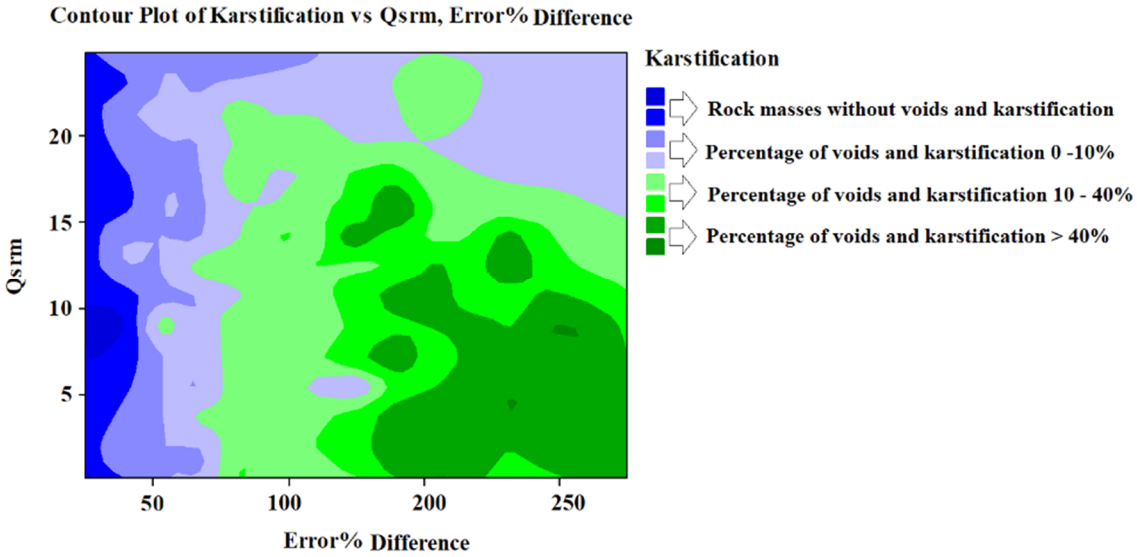

Figure 11. Contour map for the values of Q_{srm}, difference of error percentage and karstification.

3.2. Data analysis by fuzzy methods

The use of indirect methods in predicting rock mass properties, especially in lime rock, is always associated with ambiguities and uncertainty. So far, extensive studies have been done on the effectiveness of fuzzy methods to resolve many ambiguities and solve the problem in rock engineering. One of the first attempts to use the fuzzy logic theory of rock mechanics and the use of Q classification system was the research work

done by Nguyen and Ashworth [24]. Juang and Lee [25] used fuzzy methods for prediction of rock mass classifications such as RMR. Fuzzy models also improved by Yao et al. [26], Wu et al. [27], and Clouse [28] have also predicted the rock mass and seismic data.

Many comprehensive researches have also conducted the use of fuzzy principles in engineering geology [29-35]. The Fuzzy Logic Principles introduced by Zade [36] are the best means of controlling uncertainty in data. The first two phases of the fuzzy logic principle included fuzzy input data and then the use of fuzzy functions for analyzing fuzzy data. To convert non-fuzzy sets to fuzzy, several functions were used as membership functions (MFs). In the after-phase of fuzzyfying of the data, in order to establish a logical relationship between inputs and outputs, several conditional rules and algorithms are required [37].

In this study, Sugeno's fuzzy algorithm [38] was chosen to predict the Q_{srm} system with fuzzy sets. This algorithm is the most practical fuzzy algorithm in rock engineering. The general principles of the Sugeno fuzzy model in this research work are as follow:

If Input 1 = x AND (OR) Input 2 = y, then Output is $Z_i = a_i x_i + b_i y_i + k_i$

where a, b, and k are the parameters presented by matrices derived from FIS. It means that x_i is V_p and y_i is ER for each section. The final output of a fuzzy model, in fact, the average of all outputs obtained using the rules, was calculated by Equation (4).

$$Final-Output = \sum_{i=1}^{N} Z_i \left(\frac{Wt_i}{\sum Wt_i}\right) \quad (4)$$

The Z_i output is weighed from each law with a value of W. Most law-based systems include more than one rule. Finally, the result should be the aggregation of the results obtained from the various fuzzy functions. There are two simple methods for aggregation of results. In general, the common and differentiated systems of rules can be combined using the AND and OR functions [39].

MFs designed here are, in fact, simple and linear functions, whose coefficient of functions were derived from a matrix m × n in the model calculations. Each column of this matrix is the physical parameters of the MF output, and each row is equivalent to an MF. In this research work, for the Q_{srm} evaluation, 32 rules were made and a specific FIS model was presented for the Q_{srm} evaluation (Figure 12). The model designed to estimate Q_{srm} after 35 training steps resulted in at least an error.

4. Evaluation of models

To test the FIS model, the predicted values in the TH6-TH10-TH8 and TH5-TH8-TH9 sections were converted into 3D layers in ArcGIS using the spatial data interpolation methods. Figure 13 shows the Q_{srm} indicator information layers predicted by the FIS model and measured values. As shown in this figure, the information layers obtained from the FIS models have a good prediction of Q_{srm}, and the measured and predicted values are close to each other.

In addition, to check the accuracy and compare the results between the FIS and statistical methods, the R^2, Mean Absolute Deviation (MAD) [40], Variance Accounted For (VAF), and Root Mean Square Errors (RMSE) were calculated [41, 42] (see Equations 5-7).

$$VAF = \left(1 - \frac{\text{var}(y - y')}{\text{var}(y)}\right) \times 100 \quad (5)$$

$$MAD = \frac{\sum_{t=1}^{n} \left| y - mediany' \right|}{n} \quad (6)$$

$$RMSE = \sqrt{\frac{1}{N} \sum_{i=1}^{N} (y - y')^2} \quad (7)$$

where y and y' correspond, respectively, to the actual values measured relative to the rock mass quality data and the values obtained from the models. Here, R^2 is used to evaluate the relationship between the predicted and measured values (real), while VAF, MAD, and RMSE are used to compare the FIS results with different methods. As shown in Figures 10 and 14, the coefficients of determination were 0.67 and 0.86, respectively, for the regression analyses and FIS models.

Table 1 shows the results of VAF, MAPE, and RMSE for the regression analyses and FIS models. As shown, geophysical parameters in estimating Q_{srm} using the fuzzy method show a better performance than the other models used in this research work.

Range of V_p	Very Low	Low	Moderate	High	Very High
	<2.5	2.5-3.5	3.5-4	4-5	>5
fuzzy Range	0-0.2	0.2-0.4	0.4-0.6	0.6-0.8	0.8-1

Range of ER	Extremely Low	Very Low	Low	Moderate	High	Very High	Extremely High
	<200	200-500	500-800	800-1100	1100-1400	1400-1800	>1800
fuzzy Range	0-0.142	0.142-0.285	0.285-0.427	0.427-0.569	0.569-0.717	0.717-0.854	0.854-1

Range of Q_{srm}	Extremely Poor	Very Poor	Poor	Fair	Good	Very Good
	40-100	10-40	4-10	1-4	0.01-1	0.01-0. 1
fuzzy Range	0-0.166	0.166-0.333	0.333-0.5	0.5-0.666	0.666-0.833	0.833-1

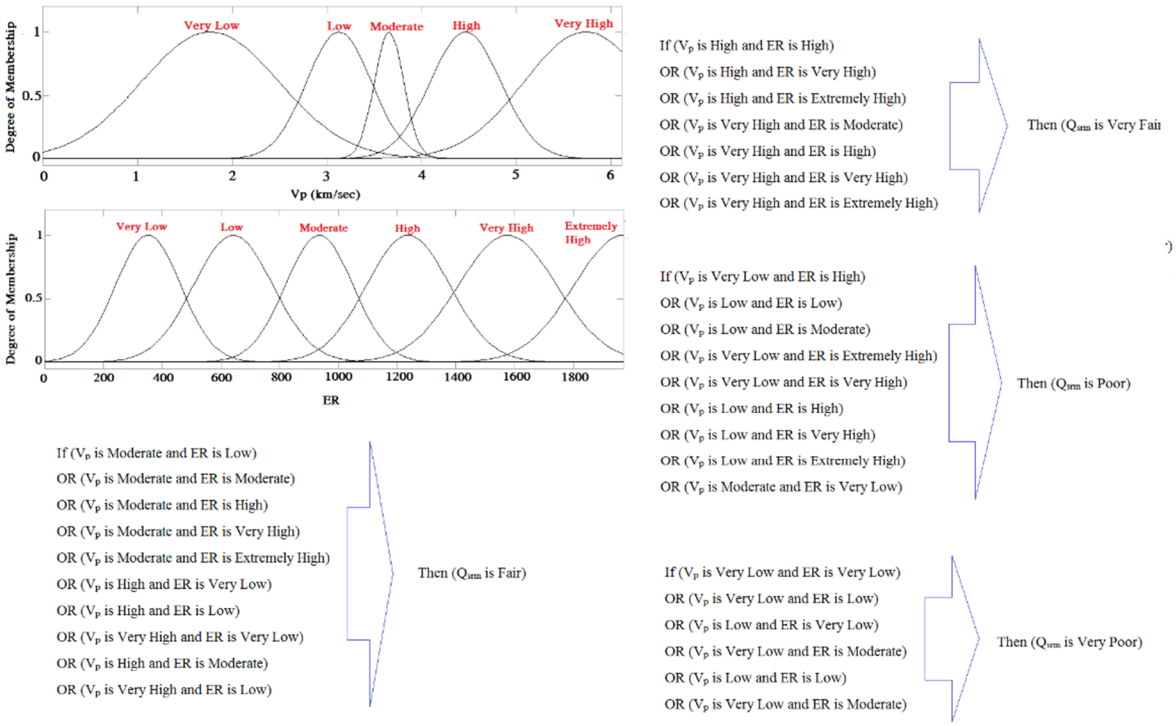

Figure 12. FIS model presented for estimating of Q_{srm} .

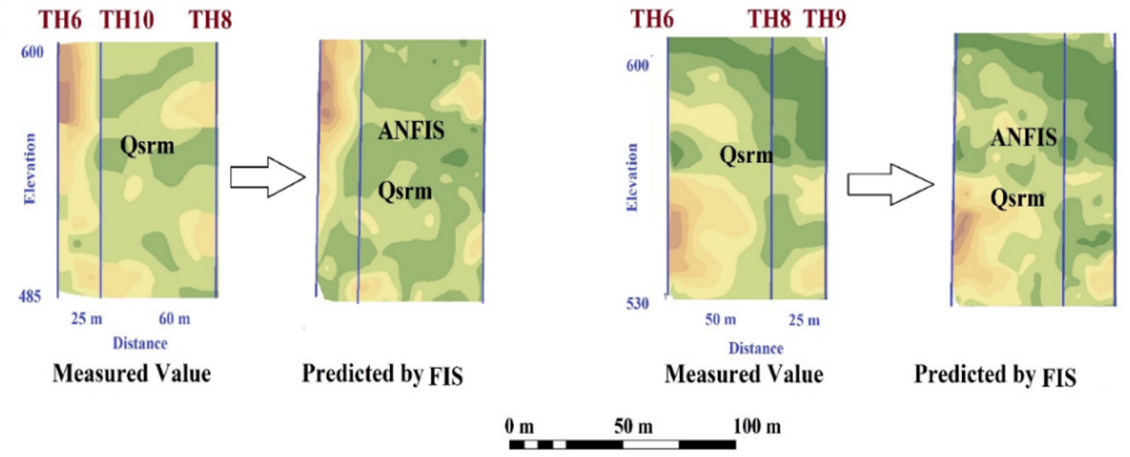

Figure 13. Raster layers of measured and predicted Q_{srm} by FIS model (data used for testing of models).

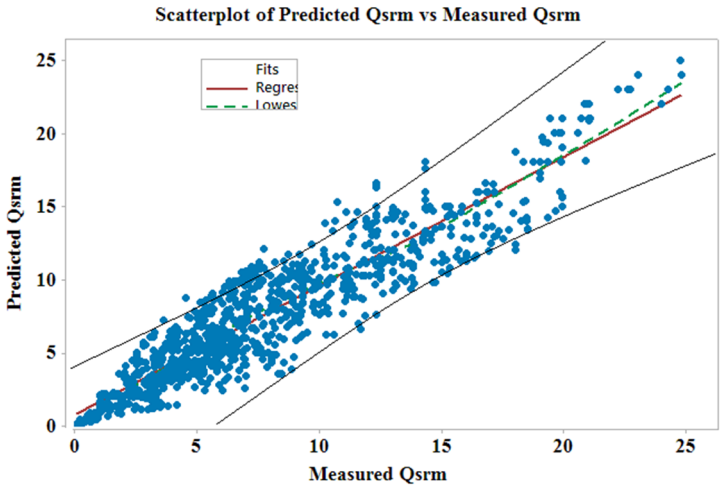

Figure 14. Relation between the predicted values with FIS and measured in-situ Q_{srm} values (R^2= 0.86).

Table 1. Results of R^2, MAD, MAPE and RMSE for regression analysis and fuzzy model.

Model	Predicted parameter	R^2	RMSE (%)	MAD	VAF (%)
Best regression	Q	0.48	37.856	3.8	25.36
Best regression	Q_{srm}	0.67	12.354	2.9	89.23
Fuzzy Method	Q_{srm}	0.86	6.63	2.1	95.35

5. Conclusions

The present work focused on the seismic and electrical parameters used to predict the quality of the Asmari limestone mass. The following conclusions can be extracted from the current work:

The mean values for Q with ER and V_p are related to a multivariable equation with a coefficient of 0.48 and the mean values of Q_{srm} with the equation with the best coefficient of 0.67. Since Q_{srm} considers a wide range of rock mass properties including cavities and layering, generally, the prediction of Q_{srm} by combining the geophysical parameters has a higher coefficient of determination and less error than prediction of Q.

In this work, fuzzy methods were used to develop predictive models for predicting Q_{srm}. R^2, VAF, MAD, and RMSE were 0.86, 95.35, 2.1, and 6.63, respectively, for the FIS model. Therefore, the results of the FIS model were closer to the actual Q_{srm} values. In fact, the reason for this is the use of qualitative boundaries in the fuzzy model, which is closer to the nature of the problem. In addition, comparing the values for R^2, VAF, MAD, and RMSE of the equations obtained from the regression analysis and FIS techniques show that the approaches using FIS for predicting Q_{srm} are much more reliable than multiple regressions. In addition, by increasing the degree of karstification of rock mass, the effectiveness of the geophysical parameters in estimating the Q_{srm} index increases with respect to other classifications studied due to the role of cavities in this classification. The results obtained in this work can be used for each region with similar geological conditions but a similar method can be used in other areas.

References

[1]. Deere, D.U. (1963). Technical description of rock cores for engineering purposes, rock mechanic and engineering geology. Journal of Rock Mechanics and Engineering Geology.1: 16-22.

[2]. Bieniawski, Z.T. (1973). Engineering classification of jointed rock masses, Trans S. Afr. Inst. Civ. Engrs. 15: 335-344.

[3]. Barton, N., Lien, R. and Lunde, J. (1974). Engineering classification of rock masses for the design of tunnel support. Journal of Rock Mechanics engineering. 6 (4): 189-236.

[4]. Carrozzo, M.T., Leucci, G., Margiotta, S., Mazzone, F. and Negri, S. (2008). Integrated geophysical and geological investigations applied to sedimentary rock mass characterization. Lecce, Italy, university of Salento, Department of Science and Material. Annals of geophysics. 51 (1): 191-202.

[5]. Lapenna, V., Lorenzo, P., Perrone, A., Piscitelli, S., Sdao, F. and Rizzo, E. (2003). High-resolution

geoelectrical tomographies in the study of Giarrossa landslide (southern Italy). Bulletin of Engineering Geology and the Environment. 62: 259-268.

[6]. Hemmati Nourani, M., Taheri Moghadder, M. and Safari, M. (2017). Classification and assessment of rock mass parameters in Choghart iron mine using P-wave velocity. Journal of Rock Mechanics and Geotechnical Engineering. 9 (2): 318-328

[7]. Azwin, I.N., Saad, R., Saidin, M., Nordiana, M.M., Bery, A.A. and Hidayah, I.N.E. (2015). Combined analysis of 2-D electrical resistivity, seismic refraction and geotechnical investigations for Bukit Bunuh complex crater. In IOP Conference Series: Earth and Environmental Science (Vol. 23, No. 1, p. 012013). IOP Publishing.

[8]. Telford, W.M, Geldart, L.P. and Sheriff, R.E. (1990). Applied geophysics. Cambridge University Press, Cambridge, UK.

[9]. Sojren, B., Ovsthus, A. and Sandberg, J. (1979). Seismic classification of rock mass qualities. Geophysics Prospect. 27: 409-422.

[10]. Boadu, F.K. and Long, T.L. (1996). Effects of fractures on seismic wave velocity and attenuation. International Journal of Geophysical. 127: 86-110.

[11]. Boadu, F.K. (2000). Hydraulic conductivity of soils from grain-size distribution: new models. Journal of Geotechnical and Environmental Engineering. 126: 739-746.

[12]. Barton, N. (2007). Rock quality, seismic velocity, attenuation and anisotropy. London: Taylor& Francis Group. pp 19-48.

[13]. Rudman, A.J, Blake, J.F. and Biggs, M.E. (1975). Transformation of resistivity to pseudo-velocity logs. Journal of American Association of Petroleum Geologists. 59: 1151-1165.

[14]. Dutta, N.P. (1984). Seismic refraction method to study the foundation rock of a Dam. Journal of Geophysical Prospecting. 32: 1103-1110.

[15]. Cardarelli, E., Marrone, C. and Orlando, L. (2006). Evaluation of tunnel stability using integrated geophysical methods. Journal of Applied Geophysics. 52 (2-3): 93-102.

[16]. Leucci, G. and Giorgi, L.D. (2006). Experimental studies on the effects of fracture on the P and S wave velocity propagation in sedimentary rock ("Calcarenite Del Salento"). Journal of Engineering Geology. 84 (3-4): 130-142.

[17]. Kearey, P., Brooks, M. and Hill, I. (2013). An introduction to geophysical exploration. Blackwell, London.

[18]. MahabGhods Consulting Engineers. (2009). Engineering geology report on Seymareh dam. Tehran, Iran.

[19]. Iran Water and Power Resourced Development Co. (2007). Final Report of Rock Mechanics of Karun 2 Dam. Tehran, Iran.

[20]. Alavi, M. (2004). Regional stratigraphy of the Zagros fold-thrust belt of Iran and its preforland evaluation. American Journal of Science. 304: 1-20.

[21]. Koleini, M. (2012). Engineering geological assessment and rock mass characterization of the Asmari formation (Zagros range) as large dam foundation rocks in southwestern Iran. PhD. Thesis, University of Pretoria, South Africa.

[22]. Karimi, H. and Tavakkoli, M. (2007). Assessment of the appeared water origin in the water tunnel of powerhouse of Seymareh dam, Ilam. Journal of Engineering Geology. 2 (1): 23-30.

[23]. Iran Water and Power Resourced Development Co. (2012). Final Report of Rock geophysical study of Karun 2 Dam.

[24]. Nguyen, V.U. and Ashworth, E.A. (1985). Rock mass classification by fuzzy sets. In: 26th US Symposium on Rock Mechanics, RapidnCity, SD. pp. 937-945.

[25]. Juang, C.H. and Lee, D.H. (1990). Rock mass classification using fuzzy sets. Tenth Southeast Asian Geotechnical Conference. Chinese Institute of Civil and Hydraulic Engineering, Taipei. pp. 309-314.

[26]. Yao, Y., Li, X. and Yuan, Z. (1999). Tool wear detection with fuzzy classification and wavelet fuzzy neural network. International Journal of Machine Tools Manufacture. 39: 1525-1538.

[27]. Wu, C., Hao, H. and Zhou, Y. (1999). Fuzzy-random probabilistic analysis of rock mass responses to explosive loads. Journal of Computer and Geotechnics. 25: 205-225.

[28]. Klose, C.D. (2002). Fuzzy rule-based expert system for short-range seismic prediction. Journal of Computer and Geoscience. 28: 377-386.

[29]. Gokceoglu, C., Yesilnacar, E., Sonmez, H. and Kayabasi, A. (2004). A neuro-fuzzy model for modulus of deformation of jointed rock masses. Journal of Computers and Geotechnics. 31 (5): 375-383.

[30]. Fişne, A., Kuzu, C. and Hüdaverdi, T. (2011). Prediction of environmental impacts of quarry blasting operation using fuzzy logic. Environmental monitoring and assessment. 174 (1-4): 461-470.

[31]. Ghasemi, E., Ataei, M. and Shahriar, K. (2011). Prediction of roof fall rate in coal mines using fuzzy logic. Proceedings of the 30th International Conference on Ground Control in Mining, University of West Virginia, Morgantown, WV. pp.186-191.

[32]. Ghasemi, E., Ataei, M. and Hashemolhosseini, H. (2013). Development of a fuzzy model for predicting ground vibration caused by rock blasting in surface

mining. Journal of Vibration and Control. 19 (5): 755-770.

[33]. Jalalifar, H., Mojedifar, S. and Sahebi, A. A. (2014). Prediction of rock mass rating using fuzzy logic and multi-variable RMR regression model. International Journal of Mining Science and Technology. 24 (2): 237-244.

[34]. Mosadeghi, R., Warnken, J., Tomlinson, R. and Mirfenderesk, H. (2015). Comparison of Fuzzy-AHP and AHP in a spatial multi-criteria decision-making model for urban land-use planning. Journal of Computers Environment and urban systems. 49: 54-65.

[35]. Feizi, F., Ramezanali, A.K. and Mansouri, E. (2017). Calcic iron skarn prospectively mapping based on fuzzy AHP method, a case study in Varan area, Markazi province. Journal of Geoscience. 21: 123-126.

[36]. Zadeh, L.A. (1973). Outline of a new approach to the analysis of complex systems and decision 431 processes, IEEE Transactions on Systems Man and Cybernetics. 3: 28-44.

[37]. Gustafson, D. and Kessel, W. (1978). Fuzzy clustering with a fuzzy covariance matrix. In 1978 IEEE conference on decision and control including the 17th symposium on adaptive processes. 17: 761-766.

[38]. Sugeno, M. (1985). Industrial applications of fuzzy control. New York, USA. Elsevier Science Pub. Co. 269 P.

[39]. Ross, T.J. (1995). Fuzzy logic with engineering applications. McGraw-Hill, New York. 600 P.

[40]. Fildes, R. and Goodwin, P. (2007). Against your better judgment? How organizations can improve their use of management judgment in forecasting. Interfaces. 37: 570-576.

[41]. Alvarez Grima, M. and Babuska, R. (1999). Fuzzy model for the prediction of unconfined compressive strength of rock samples. International Journal of Rock Mechanics and Mining Sciences. 36: 339-349.

[42]. Finol, J., Guo, Y.K. and Jing, X.D. (2001). A rule based fuzzy model for the prediction of petro physical rock parameters. Journal of Petroleum Science and Engineering. 29 (2): 97-113.

کارایی سرعت موج لرزه‌ای و مقاومت الکتریکی در ارزیابی شاخص‌های کیفیت توده سنگ (Q و Q_{srm}) (مطالعه موردی: سازند آسماری، جنوب غربی ایران)

سید محمود فاطمی عقداء*، مهدی کیانپور و مهدی تلخابلو

گروه زمین‌شناسی مهندسی، دانشگاه خوارزمی، ایران

ارسال ۲۰۱۹/۲/۴، پذیرش ۲۰۱۹/۳/۹

* نویسنده مسئول مکاتبات: fatemi@khu.ac.ir

چکیده:

در این پژوهش، رابطه پارامترهای سرعت موج فشاری (V_p) و مقاومت الکتریکی (ER) با شاخص‌های کیفیت توده سنگ شامل طبقه‌بندی کیفی توده سنگ (Q) و سیستم اصلاح شده برای سنگ‌های رسوبی، به نام Q_{srm} مورد بررسی قرار گرفته است. برای به دست آوردن مدل‌های پیش‌بینی کننده، حدود ۱۲۰۰ دسته داده از مقاطع حفاری شده در سدهای سمیره (SDS) و کارون ۲ (KDS) در سازند آسماری، جنوب غربی ایران تهیه شد. برای مطالعه روابط موجود بین پارامترهای ژئوفیزیک و کیفیت توده سنگ از روش‌های آماری و فازی استفاده شده است. از آنجا که در طبقه‌بندی Q_{srm} علاوه بر پارامترهای مورد استفاده در طبقه‌بندی Q، وجود حفرات، لایه‌بندی و بافت توده سنگ نیز در نظر گرفته می‌شود، بنابراین این طبقه‌بندی توصیف مناسب‌تری از توده سنگ ارائه داده و با پارامترهای V_p و ER رابطه نزدیکی نشان می‌دهد. معادلات به دست آمده برای پیش‌بینی Q و Q_{srm} به ترتیب دارای ضرایب تعیین ۰/۴۸ و ۰/۶۷ و برای Q_{srm} محاسبه شده از مدل فازی، ضریب تعیین ۰/۸۶ به دست آمد. در نهایت، انحراف مطلق میانگین (MAD)، واریانس محاسبه شده (VAF) و جذر میانگین مربعات خطا (RMSE) برای ارزیابی عملکرد مدل‌های آماری و فازی مورد استفاده قرار گرفت. نتایج به دست آمده از خطاهای محاسبه شده نیز نشان داد که مدل‌های فازی دارای کارایی مناسبی هستند، زیرا دقت خوبی برای پیش‌بینی Q_{srm} دارند. علاوه بر آن، با افزایش درجه کارستی شدن سنگ، کارایی پارامترهای ژئوفیزیکی برای تخمین Q به شدت کاهش می‌یابد که دلیل آن نادیده گرفتن وجود حفرات در این طبقه‌بندی است.

کلمات کلیدی: شاخص کیفیت توده سنگ رسوبی، آهک آسماری، روش ژئوفیزیکی، کارستی شدن، معادلات تجربی، سیستم استنتاج فازی.